Solid-catalyzed Reaction in a Fluidized Bed

W. K. LEWIS, E. R. GILLILAND, and WERNER GLASS

Massachusetts Institute of Technology, Cambridge, Massachusetts

Results are presented for the solid-catalyzed hydrogenation of ethylene in fixed and fluidized beds. The effect of gas velocity, bed height, catalyst activity, particle size, and internal baffles on fluidized reactor efficiency are given, and Equations derived from a simplified mathematical model correlate the data.

The success of the fluidized solid technique for the catalytic cracking of petroleum fractions led to its consideration for and application to many solid-vapor reactions encountered in the chemical and petroleum industries. The results of laboratory studies and of the use of large-scale equipment indicated that while the units had the advantages of uniformity of temperature and the ability to circulate the solid rapidly and thereby to maintain an enthalpy balance or catalyst activity, they had certain deficiencies from the viewpoint of gas-solid contacting. The relatively uniform temperature obtained is a result of the rapid solid circulation within the reactor, which results in some back mixing of the vapor. A sizable fraction of the vapor flows through the bed in gas pockets or bubbles, resulting in poor contact between the solid and gas. These factors all tend to lower the over-all reaction rate per unit of solid present that can be obtained in a fluidized bed. The interaction of these and other phenomena makes the quantitative design of fluidized reactors difficult. This study was undertaken to gain further insights into fluid-bed behavior.

Various investigators have attempted to isolate the factors affecting fluid-bed behavior for individual study. Bart (*2*), Girouard (*8*), Reman (*16*), Singer *et al.* (*20*), and others have reported on solid-mixing studies. Both eddy diffusivity and directed flow-pattern concepts were used to interpret the data. Askins *et al.* (*1*), Danckwerts *et al.* (*5*), Gilliland and Mason (*6*), Handlos *et al.* (*10*), and Reman (*16*), studying gas mixing in fluidized beds, concluded that gas back mixing is present but, at least in laboratory-sized reactors, is not very extensive. Gilliland, Mason, and Oliver (*7*) found that gas bypassing was more of a problem than gas back mixing. Such gas-solid heat or mass transfer experiments as, for example, those of Chu *et al.* (*4*), Hsu and Molstad (*12*), and Heertjes (*11*) showed that physical equilibrium between gas and solid was very readily obtained.

Fluid bed behavior can also be studied in another manner: (a) use a fluidized bed to carry out a solid-catalyzed reaction that has a known rate equation. (*b*) determine the over-all conversion when the reaction proceeds under various conditions, and (*c*) synthesize a "model" that could account for the observed results. This is the method used in this work to determine the efficiency of fluidized beds as chemical reactors.

A solid-catalized reaction that has a first-order rate equation was carried out in a 2.05-in. I.D. fluidized bed. To determine the catalyst activity (that is, the constant in the rate equation), the reaction was also carried out over a sample of the particular catalyst in question in a catalyst tester. This tester was an approximately isothermal fixed-bed reactor where piston flow of the gas and zero horizontal concentration gradients were assumed. Shen and Johnstone (*19*) and Mathis and Watson (*14*) have reported on similar studies. Their results are discussed later.

EXPERIMENTAL PROGRAM

Details of the program are given in reference *9*.

Reaction Used

The reaction used for this study was the hydrogenation of ethylene catalyzed by a nickel-coated cracking catalyst:

$$C_2H_4 + H_2 \xrightarrow{Ni} C_2H_6$$

Reaction occurred with a large excess of ethylene present. This facilitated near-isothermal operation and permitted smooth fluidization with only very small gas shrinkage in the bed. Inlet stream composition to the fluidized reactor averaged about 10% hydrogen, 90% ethylene. Feed to the fixed-bed catalyst tester averaged 5% hydrogen, 95% ethylene. Temperature and pressure averaged 235°F., 77 cm. Hg abs. Auxiliary batch experiments, detailed below, showed that under these conditions the reaction was first order in hydrogen, as predicted by several equations in the literature (*3*, *17*, etc.). Moreover, at these conditions the reverse reaction is negligible and the apparent energy of activation is very low, being given as 0 to 4 kcal./g. mole (*13*, *17*, etc.).

Determination of Reaction Order

A sample of the ethylene-hydrogen reaction mixture was repeatedly passed from one analytical gas burette, over a differential bed of catalyst maintained at reaction temperature, into another gas burette. The differential bed contained less than 50-mg. catalyst. The entire experiment was performed at nearly constant pressure. For each pass the duration and the volume of gas remaining was recorded. In due course no more shrinkage occurred. For such an experiment it can readily be shown (*9*) that if the reaction is first order in hydrogen,

$$V_c \ln (V_{h0}/V_h) + (V_{h0} - V_h) = K'mR'T'\theta$$

and if second order,

$$V_c^2\left(\frac{1}{V_h} - \frac{1}{V_{h0}}\right) + 2V_c \ln \frac{V_{h0}}{V_h} + (V_{h0} - V_h) = K''PmR'T'\theta$$

Werner Glass is with Esso Research and Engineering Company, Linden, New Jersey.

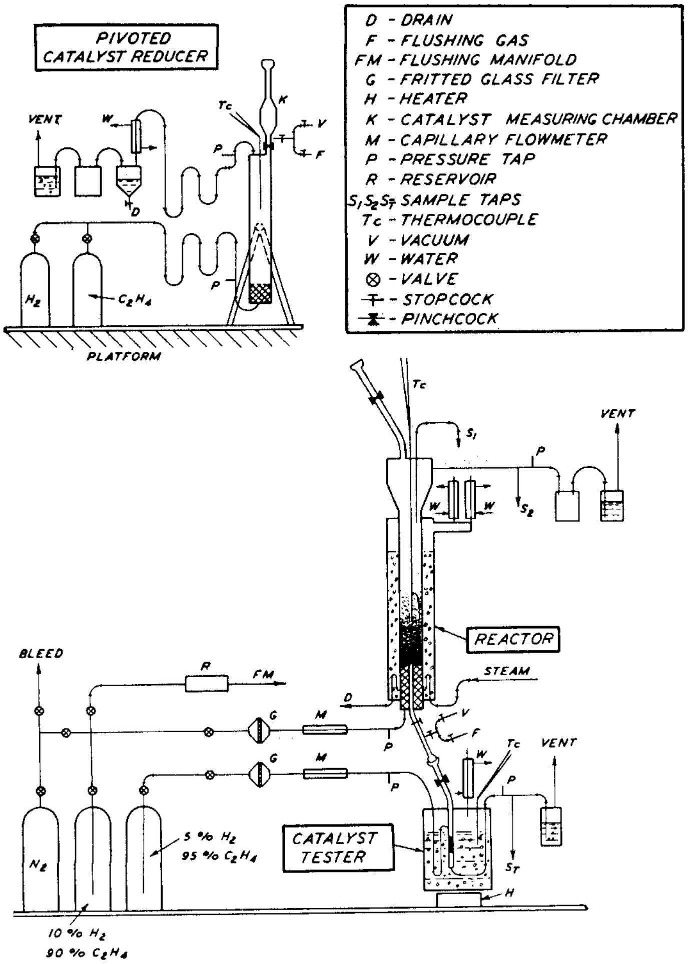

Fig. 1. Apparatus, schematic.

Table 1 lists values of K' and K'' calculated for a typical run. K' is seen to be constant enough to show that a first-order rate equation was acceptable.

Solids Used

The solid fluidized consisted primarily of the −100- + 140-mesh fraction (average particle diameter D_p:122 μ) of microspheroidal Aerocat (MS-A) cracking catalyst, which was treated to carry 2.5 or 4 wt. % either of nickel or of catalytically inactive additional alumina. Table 2 lists some properties of this solid. Some work was also done with the −65- + 80-mesh (average D_p:188 μ) and −170- + 200-mesh (average D_p:80 μ) fractions of similarly impregnated alumina.

Equipment

A flow sheet for the experimental equipment is shown in Figure 1. The equipment train consisted of three main parts.

Table 1. Determination of Reaction Order

Reaction time, sec.	First-order, K', × 10^6	Second order, K'', × 10^6
136	3.22	0.45
173	2.90	0.53
258	3.19	0.72
306	3.17	0.80
434	3.15	1.07
513	3.18	1.33
616	3.13	1.71
717	3.11	2.25
880	3.17	3.87
1,142	3.33	11.5

Pivoted Catalyst Reducer

This served to prepare catalytically active solid (MS-A carrying nickel) from a charge of MS-A carrying nickel oxide. Reduction took place by fluidizing with hydrogen at about 750°F. After reduction the charge was cooled to about 235°F., was fluidized with ethylene, and then, by pivoting of the catalyst reducer, was allowed to drop into the reactor.

Fluidized Reactor

This consisted of a 4-ft. length of 2.05-in. I.D. Pyrex tubing. A boiling-water jacket helped to maintain the desired reaction temperature. A solids disengaging section and a packed gas-inlet section were also provided.

A 325-mesh on 40-mesh stainless steel screen sandwich supported the fluidized bed. A plug normally sitting on a ¼-in. hole in these screens could be raised to permit a catalyst sample to fall into the catalyst tester below. A probe carrying a pair of thermocouples, one at the axis and one at the wall, could be inserted in the bed.

Some runs were made with a multiple baffle temporarily inserted in the bed. This baffle consisted of twelve horizontal 2-in. circles of 6-mesh stainless steel screen soldered at 2-in. intervals onto an axially located supporting tube.

Catalyst Tester

Samples of the solid being fluidized were withdrawn from the fluidized bed into a fixed-bed catalyst tester. The section of the tester in which the fixed bed was located consisted of a flattened 3-in. length

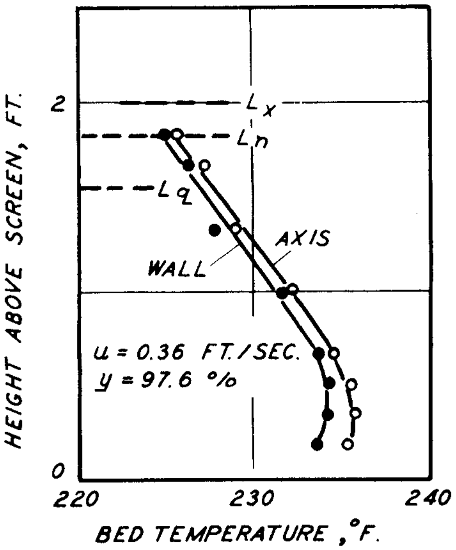

Fig. 2. Temperature profile.

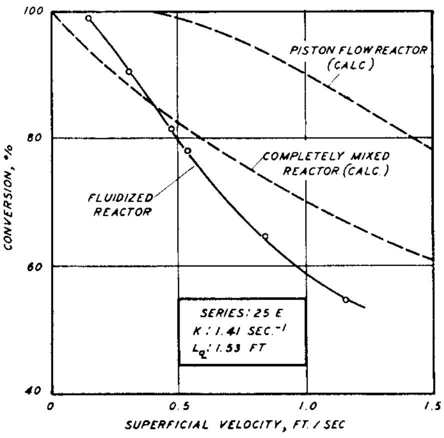

Fig. 3. Conversion vs. velocity.

Table 2. Properties of −100- + 140-Mesh Solid

Average particle diameter, (for equal surface/volume ratio)	122 μ
Quiescent bed density,	32 lb./cu. ft.
Quiescent gas velocity,	0.024 ft./sec.
Bed expansion factors	
Maximum, $\frac{L_x - L_q}{L_q(u - u_q)}$	1.1 sec./ft.
Minimum, $\frac{L_n - L_q}{L_q(u - u_q)}$	0.5 sec./ft.
Packed-bed thermal conductivity (in ethylene)	0.05 B.t.u./(hr.) (sq. ft.) (°F./ft.)

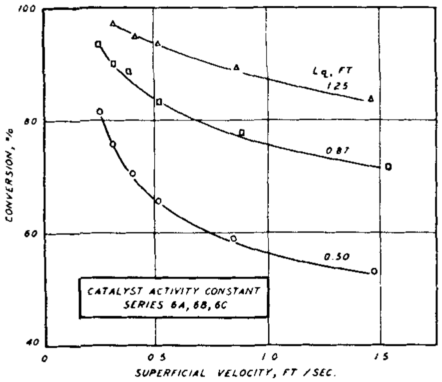

Fig. 4. Conversion vs. velocity.

of ¼-in. stainless steel tubing. The internal cross-sectional axes of this test section measured 0.11 by 0.30 in.

Procedure

A series of runs at several gas-flow rates was taken for each charge of solid in the fluidized reactor. After some series an appreciable fraction of the solid charge present was withdrawn and the next series taken on a lesser amount of the same catalyst.

Samples of catalyst were withdrawn from the fluidized reactor and the activity determined in the fixed-bed catalyst tester. The average temperature within the test section was adjusted to the average fluid-bed temperature by adjusting the calcium chloride content of the boiling liquid surrounding the tester. Several runs were made at different gas-flow rates for each sample of catalyst.

Gas samples were taken from the inlet and outlet streams of the fluidized reactor and catalyst tester. They were analyzed volumetrically for hydrogen content by being repeatedly passed over a hydrogenation catalyst until all the remaining hydrogen was used up.

RESULTS AND DISCUSSION

The results of this investigation are summarized.* Some of the data are plotted in Figures 2 to 4.

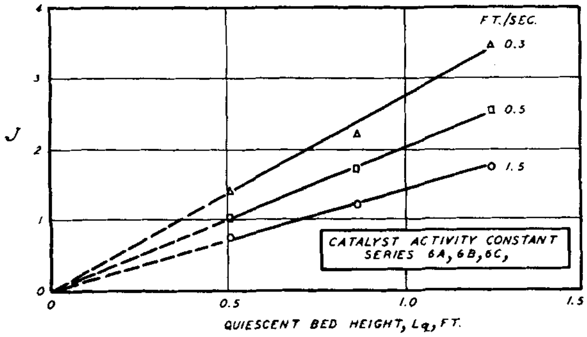

Fig. 5. *J* vs. catalyst quantity.

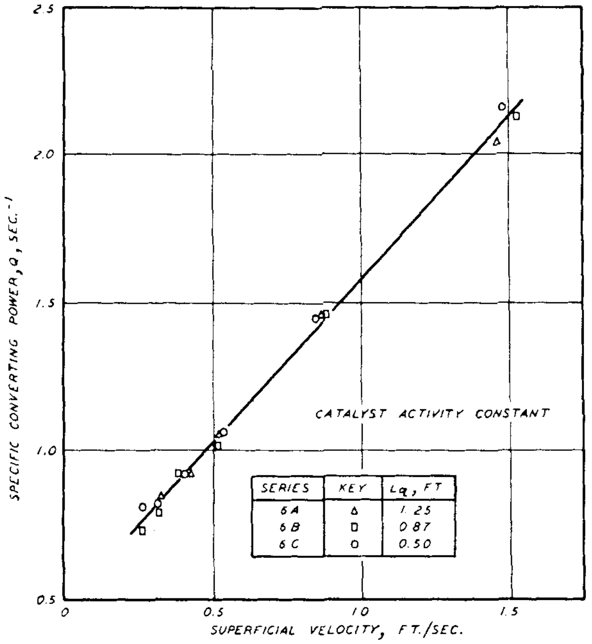

Fig. 6. Specific converting power vs. velocity.

The measurements employed in the derivations and figures are

gas-flow-rate, superficial velocity

catalyst quantity, bed height at quiescence

catalyst activity, defined by Equation (1), applicable at a given temperature and pressure:

$$-\frac{d(Auz)}{d(AL_q)} = Kz \qquad (1)$$

conversion, the fraction of hydrogen reacted

alternate measure of conversion, *J*, dimensionless. Equation (1) is readily integrated for an idealized piston-flow reactor without horizontal concentration gradients. Allowing for shrinkage, one gets

$$\frac{u}{L_q}[(1 - z_0)\ln(1/1 - y) + z_0 y] = K \qquad (2)$$

For brevity the bracketed term is defined as *J*. For zero shrinkage, hydrogenation with $z_0 \rightarrow 0$, *J* is the familiar ln $(1/1 - y)$.

specific converting power, $Q = uJ/L_q$, sec.$^{-1}$. *Q* is a measure of what the reactor accomplished per unit of solid present. For an idealized piston-flow reactor $Q = uJ/L_q = K$; that is *Q* is independent of conversion, flow rate, or catalyst

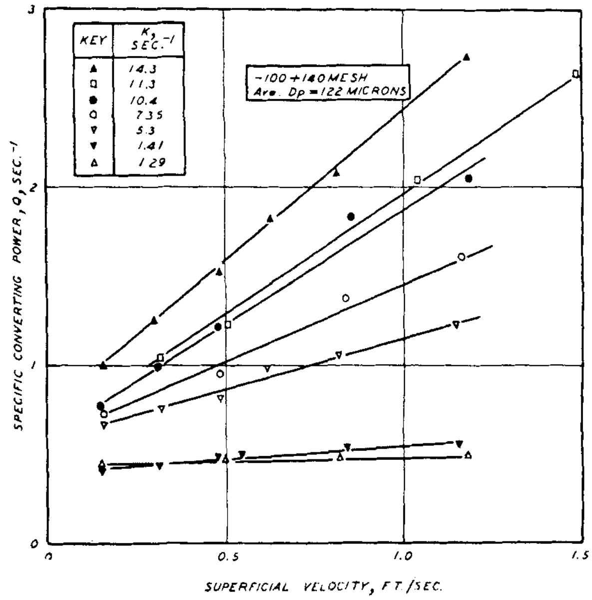

Fig. 7. Specific converting power vs. velocity.

---

*Tabular material has been deposited as document No. 5977 with the American Documentation Institute, Photoduplication Service, Library of Congress, Washington 25, D. C., and may be obtained for $1.25 for photoprints or 35-mm. microfilm.

TABLE 3. FIXED-BED RUNS—SAMPLE 25E

Run	L_q, ft.	u, ft./sec.	Conversion, %	K, sec.$^{-1}$
1	0.156	0.468	36.5	1.35
2	0.156	0.226	65.0	1.49
3	0.156	0.372	43.8	1.36
4	0.156	0.149	78.7	1.44

quantity and numerically equal to the catalyst activity. Other types of reactors will usually not make so efficient use of the catalyst and will have $Q < K$.

reactor efficiency (relative to piston flow), $E = Q/K$. For an idealized piston-flow reactor $Q = K$, and thus $E = 1$.

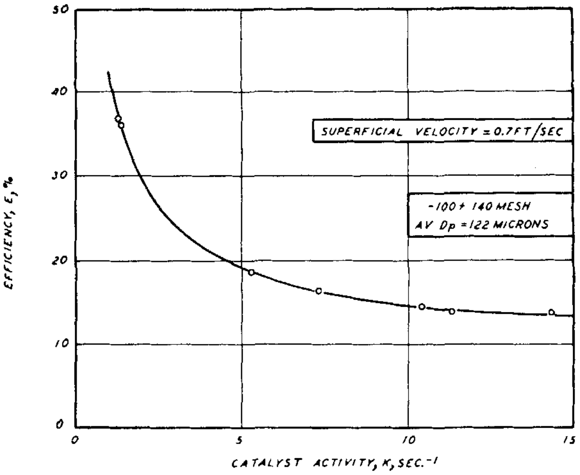

Fig. 9. Reactor efficiency vs. catalyst activity.

Range of Variables

The variables were studied in the following ranges: superficial velocity, 0.15 to 1.5 ft./sec.; quiescent bed height, 0.35 to 1.75 ft.; measured catalyst activity: 1.1 to 14.3 sec.$^{-1}$. The entire range of any one variable was not always investigated for all values of the other variables. The fluidized-bed conversions ranged from 15 to 99+%.

Fixed-Bed Runs

The conversions obtained in the fixed-bed runs for each catalyst sample were used with Equation (2) to determine the catalyst activity. Table 3 presents the data for one such sample.

Many experimental difficulties beset the determination of K, and K values were obtained for only nineteen of the sixty-three successful series of fluidized runs taken.

Fluidized-Bed Runs

The solids fluidized relatively smoothly in the 2.05-in. I.D. column used. Thermocouple traverses indicated that the temperature varied from 2° to 15°F. between the top and bottom of the bed. Radial temperature differences were small. Figure 2 shows typical profiles.

Each of the sixty-three different solid charges in the reactor resulted in a conversion vs. velocity curve. The percentage conversion always decreased with increasing velocity. In general these curves were primarily concave upward. Figure 3 shows a typical curve. Also included are the curves calculated for idealized piston flow and completely mixed reactors operating with the same quantity of the same activity catalyst as the actual fluidized bed. In all the nineteen series where K values were available for such a comparison, the fluidized-reactor conversions were less than those calculated for the corresponding piston-flow reactors. Under some reaction conditions fluidized-bed conversions were higher, and under others they were lower than those calculated for the corresponding completely mixed reactors. Thus gas back mixing alone cannot account for the lowering of conversions below those of a piston-flow reactor.

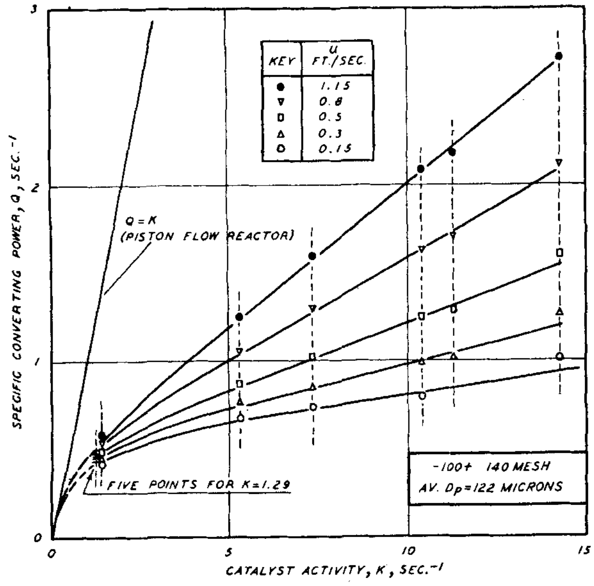

Fig. 8. Specific converting power vs. velocity.

Figure 4 shows the conversion-velocity plots obtained for a set of three series taken with varying quantities (L_q) of the same catalyst. (The actual catalyst activity was not determined for these series.) A cross plot of these data is shown in Figure 5. Instead of the conversion the quantity J (defined above) is plotted vs. L_q at various constant values of gas velocity; at any given velocity J is proportional to L_q.

A plot of specific converting power vs. velocity for this same set of three series is shown in Figure 6. At any given gas velocity the specific converting power of the fluidized reactor was independent of catalyst quantity. Six other similar sets of two or three series also showed Q independent of L_q for a given catalyst. Thus the top of a deep bed must have had the same specific converting power as the bottom.

Plots of Q vs. velocity for those series made with -100- $+140$-mesh solid for which K values were determined are presented in Figure 7. A general fan-shaped pattern may be observed; that is for high-K catalyst the Q vs. u line is quite steep, and for low-K catalyst Q does not vary greatly with velocity. For an idealized piston-flow reactor $Q = K$; that is Q is independent of velocity for a given catalyst. All the Q values obtained were considerably below the K value of the catalyst concerned.

Figure 8 presents a cross plot made from the data for the -100- $+140$-mesh solid, where Q is plotted vs. K at various constant values of velocity. Also included is the line $Q = K$ pertaining to an idealized piston-flow reactor at all velocities. The specific converting power of a fluidized bed is seen to increase continuously with increasing catalyst activity. Thus for a sufficiently active catalyst the specific converting power will be high enough to give effectively 100% conversion. (For any specified

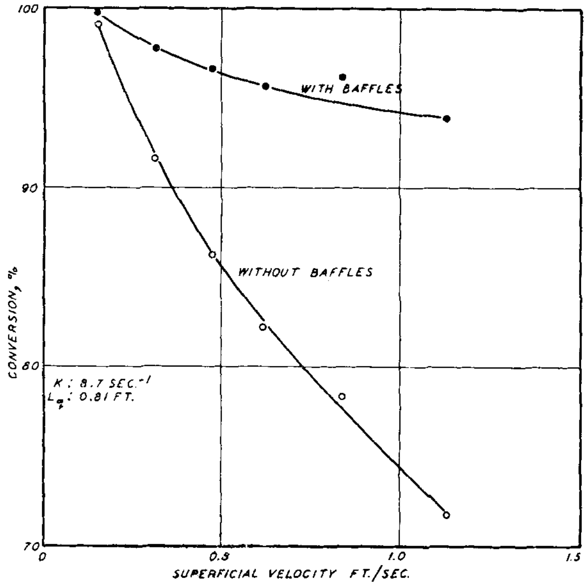

Fig. 10. Effect of baffles, conversion vs. velocity.

high-conversion level, however, far less catalyst would be needed in an idealized piston-flow reactor.) The fact that essentially complete conversion is possible shows that all the gas contacts some catalyst. This is borne out by those investigators who studied physical reactions in fluidized beds.

Figure 9 shows a cross plot of reactor efficiency $E(= Q/K)$ vs. K at a constant velocity of 0.7 ft./sec. At high enough activities the efficiency approaches a nonzero asymptotic value. The fluidized-bed efficiencies represented by the data of Figure 7 run from about 7% (at K = 14.3 sec.$^{-1}$, u = 0.15 ft./sec.) to about 39% (K = 1.29, u = 1.18).

Inserting the multiple 6-mesh screen baffle in the bed resulted in markedly increased conversions. Alternate runs were made with the same solid charge and at the same velocity with the screens either out of or in the bed. Typical results are shown in Figure 10. However operation was never truly satisfactory. The reduced solid circulation and possibly the build-up of a stagnant layer of the low-conductivity solid at the inside wall of the reactor caused very poor temperature control. The data for baffled runs were obtained while the temperature was rising continually, averaging up to 15°F. or so higher than for the unbaffled runs.

FLUID-REACTOR MODEL

Several investigators [for example, Mathis and Watson (*14*), May (*15*), and Shen and Johnstone (*19*)] have set up simplified models of flow patterns in a fluidized reactor. Appropriate integrations then predict the amount of chemical reaction that will occur in the postulated bed. In most of the proposed models the bed consists of two phases; gas flows up through one or both phases; catalyst is present in one or both phases; gas back mixing within each phase is either zero, finite, or infinite; there is interphase transfer of either the gas present or of the reacting component; and catalyst activity is independent of time and location in the bed.

A simplified model of this type for the gas flow through a fluidized bed was set up, and two extreme modifications were examined mathematically; both fitted the data equally well, with an average deviation of about 3% between actual and calculated specific converting powers. The proposed model assumes that

1. A fluidized bed consists of two phases, a gas pocket phase and an emulsion phase.
2. The gas composition at any given horizontal level is uniform within each phase but may be different in the two phases.
3. All the gas flowing up through the bed does so in the gas-pocket phase with zero back mixing.
4. The fraction a of the catalyst causes reaction to occur at a rate determined at each level of the bed by the composition of the gas in the gas-pocket phase. This a is not a function of bed level or catalyst activity.
5. The fraction $(1 - a)$ of the catalyst causes reaction to occur at a rate determined at each level of the bed by the composition of the gas in the emulsion phase.
6. Gas in the gas-pocket phase and gas in the emulsion phase undergo interchange at the rate of F cu. ft. gas/sec./cu. ft. quiescent emulsion. F is not a function of bed level or of catalyst activity.

7a. In the vertically unmixed emulsion (VUE) modification the gas in the emulsion phase is mixed in the horizontal direction only.

7b. In the completely mixed emulsion (CME) modification the emulsion-phase gas is uniform throughout the reactor.

Mathematical Description

A first-order reaction occurring without shrinkage will be considered. This would correspond to hydrogenation with $z_0 \to 0$.

The amount of catalyst in the whole bed is L_q. A horizontal slice of the bed contains dh catalyst, of which $(1 - a)dh$ catalyst sees emulsion-phase gas and adh catalyst sees gas-pocket-phase gas (Figure 11).

Reactant balances can be written for the gas in both phases.

VUE Modification

For the gas-pocket phase gas

Input	from gas stream	xu
	from emulsion	$x_eF(1 - a)dh$
Output:	to gas stream	$(x + dx)u$
	to emulsion	$xF(1 - a)dh$
	to chemical reaction	$x\ Kadh$

Equating input to output and rearranging, one gets

$$\frac{dx}{dh} + \frac{F(1 - a)(x - x_e)}{u} + \frac{aKx}{u} = 0 \qquad (3)$$

For the emulsion phase gas

Input:	from gas stream	$xF(1 - a)dh$
Output:	to gas stream	$x_eF(1 - a)dh$
	to chemical reaction	$x_eK(1 - a)dh$

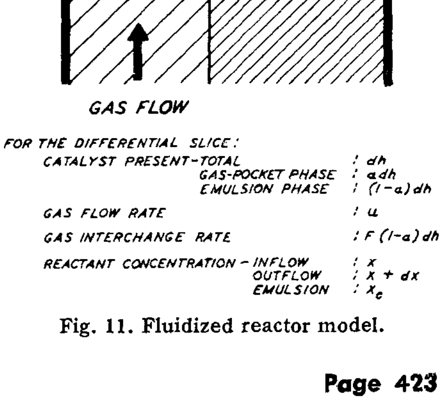

Fig. 11. Fluidized reactor model.

When one rearranges,

$$F(x - x_e) = Kx_e \qquad (4)$$

The concentration in the emulsion can be eliminated between these two equations and the resulting equation integrated by use of the boundary conditions

$$x = x_1 \quad \text{at} \quad h = 0$$

$$x = x_2 \quad \text{at} \quad h = L_q$$

and noting $y = (x_1 - x_2)/x_1$. The solution can be written

$$\ln (1/1 - y) = \frac{L_q}{u}\left[aK + \frac{1 - a}{1/K + 1/F}\right]$$

A derivation taking shrinkage into account would be unduly cumbersome. In the present study complete conversion would give only 10% shrinkage, and so the actual effect is probably small.

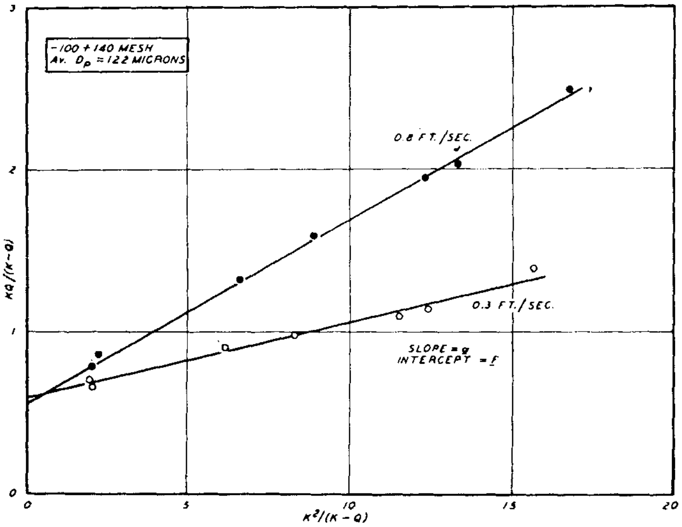

Fig. 12. Applicability of Equation (6).

This same term, ln (1/1 − y), occurs in the expression for a piston-flow reactor. There the effect of shrinkage is accounted for when

$$J \doteq (1 - z_0) \ln (1/1 - y) + z_0 y$$

replaces ln (1/1 − y). Arbitrarily this same substitution is used here. Then

$$\frac{Ju}{L_q} = Q = aK + \frac{1 - a}{1/K + 1/F} \qquad (5)$$

Dividing Equation (5) by K gives an expression for the reactor efficiency $E = Q/K$.

$$E = a + \frac{(1 - a)}{1 + K/F} = \frac{F + aK}{F + K} \qquad (6)$$

Here a can be looked at as the contribution of the gas-pocket phase and $(1 - a)/(1 + K/F)$ as that of the emulsion phase.

This VUE model corresponds to a special case (zero upflow through the emulsion) of the model proposed by Mathis and Watson (*14*)

CME Modification

Again a first-order reaction without shrinkage is considered. Here the emulsion-phase gas is uniform throughout the reactor with a reactor concentration x_e.

For a horizontal slice of the bed a reactant balance for the gas-pocket phase gas is the same as for the VUE.

$$\frac{dx}{dh} + \frac{F(1 - a)(x - x_e)}{u} + \frac{aKx}{u} = 0 \qquad (3)$$

When all the emulsion phase gas in the bed is considered,

Input: from gas stream

$$\int_0^{L_q} xF(1 - a)\, dh$$

Output: to gas stream $x_eF(1 - a)L_q$
to chemical reaction $x_eK(1 - a)L_q$

When one rearranges,

$$\int_0^{L_q} xF(1 - a)\, dh = x_e(1 - a)L_q(K + F) \qquad (7)$$

Eliminating x_e and solving with the same boundary conditions as before results in

$$\frac{1}{y} = \frac{1}{1 - \exp\left[-\left(\frac{KL_q}{u}\right)\left(a + \frac{1 - a}{K/F}\right)\right]} + \frac{1}{\left(\frac{KL_q}{u}\right)\left(1 + a\frac{K}{F}\right)\left(1 + \frac{a}{1 - a}\frac{K}{F}\right)} \qquad (8)$$

Comparison with the Data

The vertically unmixed emulsion modification (VUE) leads to Equation (5), which has Q independent of L_q. The CME solution does not lead to a Q mathematically independent of L_q. Thus at first sight the VUE appears more likely to fit the data, as experimentally Q did not vary with L_q for a given catalyst at constant velocity.

VUE Modificaton

The fit of Equation (5) for the VUE to the data can be readily checked by transformation to

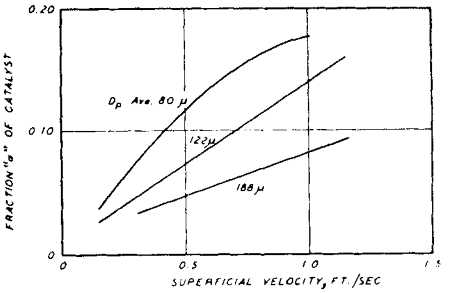

Fig. 13. Values of *a*.

$$\frac{KQ}{K - Q} = \frac{aK^2}{K - Q} + F \qquad (9)$$

A plot of $KQ/(K - Q)$ vs. $K^2/(K - Q)$ at constant gas velocity for a given particle size should give a straight line of slope a and intercept F. Figure 12 presents such plots for the −100- + 140-mesh solid at velocities of 0.3 and 0.8 ft./sec. Good straight lines are obtained. Thus at a given velocity single values of a and F will allow Equation (9) to fit the data for the seven series run with different catalyst activities.

Values of a and F obtained from the data are plotted against gas velocity in Figures 13 and 14. For any one solid a increases appreciably with velocity, and F decreases slightly. The nature of a and F will be further discussed later.

In accordance with the VUE model, the efficiency is given by

$$E = \frac{Q}{K} = a + \frac{1 - a}{1 + K/F} \qquad (6a)$$

Thus at high values of K, or with very little gas interchange, the efficiency ap-

Table 4. Comparison With Data of Shen (*18*)

	Fixed beds		Fluidized beds		
	Data				Model
Temperature, °F.	K, sec.$^{-1}$ Range	Avg.	Q, sec.$^{-1}$ Range	Avg.	Q, sec.$^{-1}$ for avg. K
700	0.00590–0.00636	0.00613	0.00555–0.00602	0.00578	0.00605
750	0.0114–0.0122	0.0118	0.0107–0.0121	0.0114	0.0115
800	0.0198–0.0212	0.0205	0.0169–0.0190	0.179	0.0194

proaches a. At very low activities or high gas-interchange rates the efficiency would approach 1, that is that of an idealized piston-flow reactor.

CME Modification

Equation (8) gives the solution for the CME model; no ready way to obtain a and F explicitly could be found.

The differences between the VUE and CME models will be considered. The VUE assumes that emulsion-phase gas is not vertically mixed and the CME assumes that it is. The VUE predicts that the reactant concentration x_e in the emulsion at any level in the bed is given by Equation (4). When one rearranges and substitutes conversions,

$$y_{e,h} = \frac{y_h + K/F}{1 + K/F}$$

Thus if K/F is large or if y is small, the emulsion-phase gas of a VUE reactor is going to be very uniform, and the conversion will be the same as in a CME reactor. This was the case in the ranges of K/F and conversions covered in the present study. The values of a and F obtained by fitting the VUE model to the data, when used in Equation (8) along with the experimental values of K, L_Q, and u, predicted conversions negligibly different from those predicted by Equation (5). These experiments were thus not able to pin down the amount of gas back mixing in the emulsion phase. The effect of any such back mixing would become important for deeper beds of less active catalyst and at high gas-interchange rates.

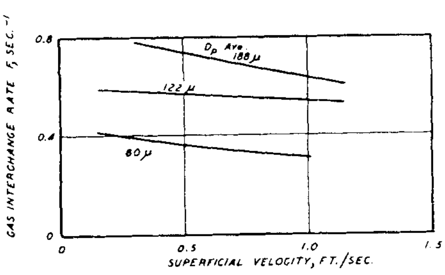

Fig. 14. Values of F.

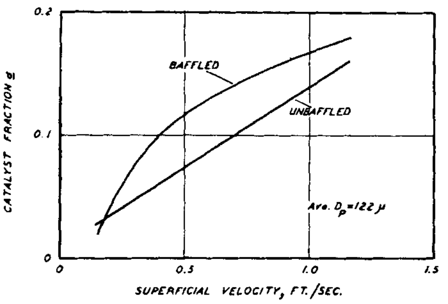

Fig. 15. Effect of baffles, values of a.

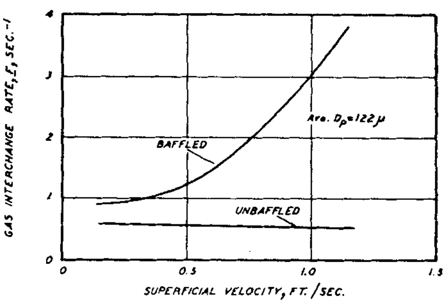

Fig. 16. Effect of baffles, values of F.

The Catalyst Fraction a

The model assumes that the fraction a of the solid differs from the rest. It alone sees the flowing gas-pocket phase gas. Slow-motion movies showed that differences between fractions of the solid exist.

Some nickeled (black) microspheres were added to a batch of normal (white) microspheres and the mixture was fluidized in a rectangular cross-section column having one plate-glass face. The entire column was tilted backward a few degrees from the vertical so that the solid flow patterns made visible by frontal illumination would be more representative of conditions within a fluidized bed.

The movie showed that the microspheres were aggregated in two distinct forms. The main part made up the emulsion proper. This emulsion phase moved around quite showly with little apparent motion of the particles relative to their immediate neighbors. A different type of solid phase existed (1) directly underneath most of the gas pockets, (2) inside the gas pockets, (3) above some of the gas pockets, and (4) between some pairs of gas pockets where one was more or less vertically above the other. In these zones the microspheres appeared to be moving rapidly, and no individual particles could be recognized. This solid may well correspond to the fraction a which the model specifies as seeing gas-pocket phase gas.

No quantitative estimate of the amount of solid present in this second phase could be made. However more solid was involved at high gas velocities than at low ones.

The Gas-Interchange Rate F

Gas interchange between gas pocket and emulsion can be assumed to occur in two main ways: (1) gas flowing from one phase to the other through the surface of the gas pockets and (2) gas being transferred along with the bulk transfer of solid from one phase to the other. At low gas rates the limited bed expansion shows that the volume of the gas-pocket phase is small. The velocity across the gas-pocket surface is probably less than at higher gas rates. The calculated gas interchange rate is however no less than at higher throughputs. If flow across the surface were the only means of interchange, extremely small gas pockets would be needed to provide enough of this surface. Postulating direct interchange of gas from one phase to the other, in conjunction with the transfer of solid, can help to account for the calculated values of F.

Effect of the Multiple Baffle

Values of a and F were obtained for runs where the multiple coarse-screen baffle was present in the fluid bed. Figures 15 and 16 show these values compared to those obtained without the screens; there was no great difference in a. Values of F, interpreted as gas interchange between gas-pocket and emulsion phases, were appreciably higher for the runs with screens in the bed; the increase ranged from about 50% at low velocities to about 600% at high velocities.

It seems plausible that the numerous coarse screens continuously break up the emulsion and thus help the transfer of gas from one phase to the other. This breakup of the emulsion can be relatively slight at lower gas velocities, where the gas pockets are small and the motion of the emulsion phase engendered by them quite gentle. At higher velocities, though, the emulsion is subjected to more violent forces and the screens will be far more restrictive; that is they will obstruct the free motion of the emulsion more. They will then cause far greater breakup of the emulsion and thus bring about greater gas interchange with the gas-pocket phase.

Comparison With Data of Shen (18)

Shen carried out fixed- and fluid-bed decomposition of nitrous oxide in a 4 ½ in.-diameter column. Air or nitrogen was used as the carrier gas. His results for −165- + 200-mesh catalyst with air as a carrier are shown in Table 4. To make comparison easier, the results are expressed in the units used here.

Shen's catalysts had very low values of K (<0.021 sec.$^{-1}$). The VUE model predicts that for such low K's the efficiency should be $> 95\%$, that is that there should be little difference between fixed and fluidized beds. That this was so is evident from his data.

Also included in Table 4 are values of Q predicted from the VUE model for the average values of K. To make the predictions, values of F and a were obtained from the present data for -170- $+$ 200-mesh catalyst. For the low velocities at which Shen's fluidized runs were made (0.025 to 0.19 ft./sec.) a was taken as 0.02 and F as 0.4 sec.$^{-1}$. Reasonably good agreement between measured and predicted Q's was obtained. However any other model that asymptotes to fixed-bed efficiency at very low conversions would fit as well.

Comparison With Data of Mathis and Watson (14)

Mathis and Watson dealkylated cumene in fixed and fluidized beds 2, 3, and 4 in. in diameter. Their results differed from those of this study in two major points:

1. Reactor efficiency reached a maximum at gas velocities of about 0.4 ft./sec. (Conversion vs. velocity curves slightly concavely downward.) This maximum was most pronounced for rather shallow beds 1 to 6 in. deep.
2. Reactor efficiency decreased as bed height increased from 1 to 12 in.

All their runs were made with the same catalyst activity. From their fixed-bed data a pseudo first-order activity of $K = 1$ sec.$^{-1}$ can be assigned as an approximation. For such a catalyst the VUE model would predict efficiencies of around 40% on the basis of F and a values obtained in the present work. The reported efficiencies ranged from about 15 to 100%. If the shallow beds of 6 in. or less are not considered, the range of efficiencies for the deeper beds decreases to 25 to 55%, with eight out of eleven runs between 35 and 45%. Thus the VUE model would be quite satisfactory for beds of about the same depth as those used in the present work.

CONCLUSIONS

1. Gas back mixing alone could not explain the difference between the conversions obtained in a fluid bed and those calculated for the corresponding idealized piston-flow reactor.
2. The efficiency of a fluid bed as a reactor for carrying out a first-order, solid-catalyzed reaction was independent of bed height. The top and bottom of a bed were equally effective.
3. The reactor efficiency increased appreciably with gas velocity for fluid beds of very active catalyst and was almost independent of velocity for beds of less active catalyst.
4. For a given particle size the reactor efficiency could be correlated by

$$E = \frac{F + aK}{F + K}$$

where F and a are functions of velocity only, with a roughly proportional to velocity and F decreasing slightly with increasing velocity. Increasing particle size raised F and lowered a.

5. The data were correlated by a simplified two-phase model where F is the gas interchange rate between emulsion and gas-pocket phases, a is the fraction of catalyst causing reaction to occur in the up-flowing gas-pocket phase gas, and $(1 - a)$ is the fraction of catalyst causing reaction to occur in the emulsion phase gas. No conclusions regarding the degree of back mixing in the emulsion could be drawn.
6. Inspection of slow motion movies qualitatively supported the division of the solid into two different fractions.
7. Gas interchange occurred as gas flow between the two phases or as bodily transfer of one phase (including the solid therein) into the other. Several coarse horizontal screens placed in the bed markedly increased this gas interchange. The effect was most pronounced at high gas rates.
8. The correlations developed agreed quite well with Mathis and Watson's data (*14*) for beds deeper than 6 in. and with the data of Shen (*18*).

ACKNOWLEDGMENT

This work was carried out as part of a research project sponsored by the Esso Research and Engineering Company. The American Cyanamid Company donated over 600 lb. of MS-A cracking catalyst. H. H. Carter prepared the drawings.

NOTATION

A = reactor cross section, sq. ft.
a = catalyst fraction causing reaction in gas-pocket phase gas
CME = completely mixed emulsion model
D_p = average particle diameter, μ
E = reactor efficiency = Q/K
F = gas-interchange rate, (cu. ft. gas/sec.)/(cu. ft. quiescent emulsion) or sec.$^{-1}$
h = variable for L_q, ft.
J = measure of conversion = $(1 - z_0) \ln (1/1 - y) + z_0 y$
K = catalyst activity, sec.$^{-1}$
K' = activity, (g. mole/sec.)/(g. cat.) (cm. Hg)
K'' = activity, (g. mole/sec.)/(g. cat.) (cm. Hg)^2
L_n = minimum bed height, ft.
L_q = quiescent bed height, ft., measure of catalyst quantity
L_x = maximum bed height, ft.
m = weight of catalyst, g.
P = pressure, cm. Hg
Q = specific converting power = uJ/L_q, sec.$^{-1}$
R' = gas constant, cc. — cm. Hg/g. mole °K.
T' = temperature of gas in measuring burette, °K.
u = superficial gas velocity, ft./sec.
u_q = quiescent velocity, ft./sec.
VUE = vertically unmixed emulsion model
V_c = residual volume, cc.
V_h = volume hydrogen at time θ, cc.
V_{h0} = volume hydrogen at zero time, cc.
x = mole-fraction reactant in gas-pocket phase gas
x_e = mole-fraction reactant in emulsion phase gas, reactor concentration
y = conversion
$y_{e,h}$ = emulsion phase-gas conversion at any level in the bed
y_h = gas-pocket phase-gas conversion at that level
z = mole fraction hydrogen
z_0 = mole fraction hydrogen in the inlet stream
θ = reaction time, sec.

LITERATURE CITED

1. Askins, J. W., G. P. Hinds, Jr., and F. Kunreuther, *Chem. Eng. Progr.*, **47**, 401 (1951).
2. Bart, Roger, thesis, Mass. Inst. Technol., Cambridge, Massachusetts (1950).
3. Beeck, Otto, *Rev. Mod. Phys.*, **17**, 61 (1945).
4. Chu, J. C., James Kalil, and W. A. Wetteroth, *Chem. Eng. Progr.*, **49**, 141 (1953).
5. Danckwerts, P. V., J. W. Jenkins, and G. Place, *Chem. Eng. Sci.*, **3**, 26 (1954).
6. Gilliland, E. R., and E. A. Mason, *Ind. Eng. Chem.*, **41**, 1191 (1949).
7. ———, and R. C. Oliver, *ibid.*, **45**, 1177 (1953).
8. Girouard, H. D., thesis, Mass. Inst. Technol., Cambridge, Massachusetts (1954).
9. Glass, Werner, thesis, Mass. Inst. Technol., Cambridge (1956).
10. Handlos, A. E., R. W. Kunstman, and D. O. Schissler, *Ind. Eng. Chem.*, **49**, 11 (1957).
11. Heertjes, P. M., H. G. J. de Boer, and A. H. de H. van Dorsser, *Chem. Eng. Sci.*, **2**, 97 (1953).
12. Hsu, C. T., and M. C. Molstad, *Ind. Eng. Chem.*, **47**, 1550 (1955).
13. Klar, Richard, *Z. physik. Chem.*, **A168**, 215 (1934).
14. Mathis, J. F., and C. C. Watson, *A.I.Ch.E. Journal*, **2**, 518 (1956).
15. May, W. G., personal communication (1954).
16. Reman, G. H., *Chem. & Ind. (London)*, Jan. 15, 46 (1955).
17. Schuster, Curt, *Z. physik. Chem.*, **B14**, 249 (1931).
18. Shen, C. Y., Ph.D. thesis, *Univ. Illinois*, Urbana, Illinois (1954).
19. Shen, C. Y., and H. F. Johnstone, *A.I.Ch.E. Journal*, **1**, 349 (1955).
20. Singer, E., D. B. Todd, and V. P. Guinn, *Ind. Eng. Chem.*, **49**, 11 (1957).

Manuscript received March 3, 1958; revision received December 31, 1958; paper accepted January 8, 1959. Paper presented at A.I.Ch.E. Chicago meeting.